Extension of the LBM to 3D fully unstructured grids

S. Ubertini[a,*], N. Rossi[a], G. Bella[a], S. Succi[b]

[a] University of Rome 'Tor Vergata', Department of Mechanical Engineering, 00133 Rome, Italy
[b] Istituto Applicazioni Calcolo, CNR, Rome, Italy

Abstract

This paper presents a compact and efficient finite-volume lattice Boltzmann formulation on three-dimensional unstructured grids based on a cell-vertex scheme. The resulting model has been tested against the laminar flow past a sphere at low Reynolds numbers.

Keywords: Lattice Boltzmann method; Unstructured grids; Finite volumes; Fluid dynamics

1. Introduction

During the last decade, the Lattice Boltzmann Method (LBM) evolved into an interesting alternative to conventional CFD methods and, due to the refinements and the extensions of the last years, it has been used to successfully compute a number of nontrivial fluid dynamics problems [1,2,3,4,5]. The main advantages of the LBM are its computational simplicity, relative locality and amenability to parallel computing. However, a recognized limitation of the original LBM is its restriction to regular, uniform lattices and this limitation becomes particularly severe whenever high local resolution is required. Over the recent years, this limitation has motivated a wide body of research to the point that today many options are available to deal with realistically complex geometries [6,7,8]. Particularly interesting options are recent attempts to formulate LB on a fully unstructured grid [8,9] using a finite-volume formulation of the cell-vertex type. In previous papers [9,10], it has been shown that the bi-dimensional implementation of this method with coarse-graining triangles tolerates significant grid distortions without showing any appreciable numerical viscosity effects at second order in the mesh size. In this work, we present the three-dimensional generalization of the Unstructured Lattice Boltzmann technique (ULBE as Unstructured Lattice Boltzmann Equation), in which geometrical flexibility is achieved at the level of coarse-graining tetrahedra. The ease and the accuracy of calculating aerodynamic forces are shown by simulating low Reynolds number fluid flows past a sphere.

* Corresponding author. Tel.: +39 06 7259 7170; Fax: +39 06 2331 0028; E-mail: stefano.ubertini@uniroma2.it

Computational Fluid and Solid Mechanics 2005
K.J. Bathe (Editor)

2. ULBE numerical formulation

The differential form of the single-time relaxation Lattice Boltzmann equation reads as follows:

$$\partial_t f_i + \vec{c}_i \cdot \vec{\partial}_x f_i = -\frac{f_i - f_i^{eq}}{\tau} \tag{1}$$

where the particle distribution function (also called population) f_i ($\vec{x}$, t) represents the amount of fluid per unit volume moving with velocity $\vec{c}_i$ at the site $\vec{x}$ and at time t. The right-hand side of Eq. (1) is the Bhatnagher-Gross-Krook (BGK) collision operator [11], which represents molecular collisions via a single-time relaxation (τ as the time-scale) toward 'local equilibrium'. The local equilibrium function f_i^{eq} depends only on the locally conserved quantities (such as mass density and momentum density) and are carefully chosen so that Galilean invariance and the Navier-Stokes equations are recovered in the limit of weak departures from f_i^{eq} [2]:

$$f_i^{eq} = \rho\omega_i \left\{ 1 + \vec{c}_i \cdot \vec{u}/c_s^2 + \frac{1}{2c_s^4}\left[(\vec{c}_i \cdot \vec{u}) - u^2\right] \right\} \tag{2}$$

where c_s is lattice sound speed.

The macroscopic local quantities may be computed at any instant during the evolution by taking the appropriate discrete velocity moments of the distribution functions:

$$\rho = \sum_i f_i \tag{3}$$

$$\vec{u} = \sum_i f_i \vec{c}_i \tag{4}$$

In order to recover faithful fluid dynamics, the set of discrete speeds must be chosen in such a way as to guarantee mass, momentum and energy conservation, as well as rotational invariance. In the present formulation we have used the nineteen-speed model (known as D3Q19 [2]) consisting of one speed-zero particle, six speed-one particles (nearest-neighbor connection to face centers) and twelve speed-two particles (particles streaming to the edge-connected neighbors).

The traditional discrete Boltzmann equation can be derived by applying an explicit finite difference scheme to Eq. (1). A square lattice is used, particles can only reside on the nodes and at each time-step move to their nearest neighbours. The corresponding kinematic shear viscosity is related to the relaxation time by $\upsilon = c_s^2\,(\tau - dt/2)$ [2].

The ULBE approach, to numerically solve Eq. (1), is instead a finite-volume scheme based on a space discretization into tetrahedral elements. To each node P of the discrete grid, we associate a set of 19 discrete populations $f_{i,}$, which represent the unknowns of the problem. The set of K tetrahedra $T_k(P)$ (see Fig. 1) which share P as a common vertex defines the finite volume Ω_P associated with node P. Referring to the generic k-th tetrahedral (Fig. 1), the point O_k is the centre of the tetrahedral, E_m are the midpoints of the edges that emanate from vertex P and S_{jl} are the centres of surfaces identified by nodes (P, N_j, N_l).

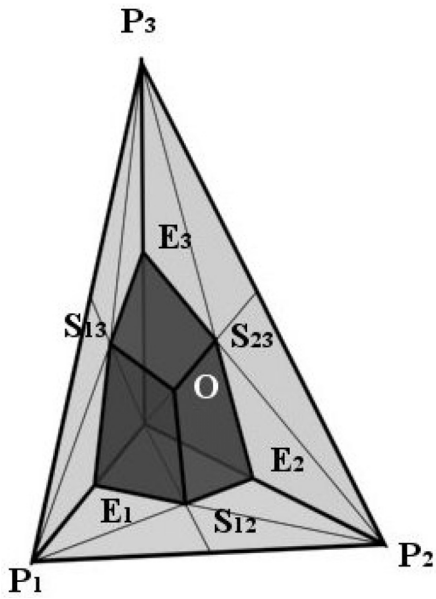

Fig. 1. Geometrical layout of the cell-vertex finite volume formulation.

Application of the Gauss theorem to each finite volume Ω_k yields the following set of ordinary differential equations:

$$\partial_t f_i(P,t) = \frac{1}{V_P}\sum_{k=0}^{K}(\Phi_{ik} - \Xi_{ik}) \tag{5}$$

where the sum k runs over the control volume Ω_P obtained by joining the centers O_k with points S_{jl} and E_m. In the above, V_P is the volume of $\Omega_P = \cup_k \Omega_k$.

Finally, Φ_{ik} denotes the flux associated with the streaming phase of the i-th population and Ξ_{ik} is the contribution of the collision arisen from the integration of the collision term $f_i - f_i^{eq}/\tau$ over the volume Ω_k.

The detailed expressions of the streaming and collision matrices S_{ik} and $C_{ik} = C_k\delta_{ik}$ give the following general form of the ULBE:

$$\partial_t f_i(P,t) = \sum_k S_{ik} f_i(P_k,t) - \frac{1}{\tau}\sum_{k=0}^{K} C_{ik}\left[f_i(P_k,t) - f_i^{eq}(P_k,t)\right] \tag{6}$$

For the time discretization it is sufficient to prescribe the size of the time-step and the solution of Eq. (6) is obtained by marching in time from the prescribed initial condition. In this work we have used the 'covolume method' to deal with both no-slip and free-slip wall boundaries [8,9]. In the covolume method, the fluxes across boundary surfaces are evaluated by explicit interpolation at the boundary surfaces.

At the inlet boundary a prescribed velocity profile is imposed, whereas constant pressure is imposed at the outlet sections. This is allowed by a straightforward three-dimensional extension of the procedure developed in [9,10], in which the computational domain is augmented with one or more buffers of uniform tetrahedra.

3. Numerical results

As a preliminary step, a three-dimensional driven laminar flow in a circular pipe has been simulated in order to measure numerical viscosity. For different values of τ varying between 0.01 and 0.001, it was found that numerical viscosity effects are within second order of accuracy in space and the constant kinematics viscosity reads as follows:

$$\upsilon = c_s^2\tau \tag{7}$$

which is exactly the expression found in two dimensions [9,10].

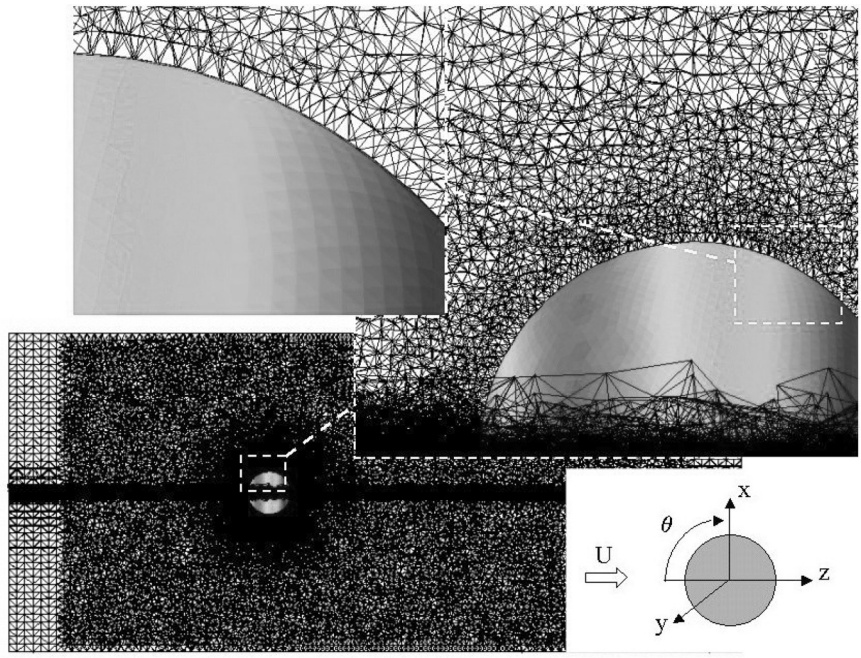

Fig. 2. Coordinate system and unstructured grid near the sphere at Re = 100.

For the validation of the present numerical method, numerical simulations of the laminar flow past a sphere ($10 < Re < 100$) and comparisons with available literature data have been performed.

The unstructured grids used in the computations consist of a number of nodes in the range 53,800–460,000 for Re = 10 and Re = 100 respectively. In Fig. 2 the latter grid and the coordinate system are shown.

Upon reaching steady-state, the drag coefficient, C_d, is measured. In a hydrodynamic (Navier-Stokes) representation, the friction contribution to drag (viscous stress tensor) requires the computation of the velocity gradients. The LB approach has the nice property that the stress tensor is locally available as a linear combination of the populations:

$$S_{ab} = \sum_i \left(c_{ia}c_{ib} - \delta_{ab}c_s^2\right) \cdot \left(f_i - f_i^{eq}\right) \quad a,b = x,y,z \qquad (8)$$

However, this property is not fully exploited in the traditional LB because the body surface does not generally lie on grid points. The advantage of ULBE is that no interpolation is required because the body surface is made of grid points. As a result, in the ULBE formulation both pressure and viscous contributions to drag are locally available.

Figure 3 shows the computed drag coefficient compared to numerical and experimental data found in the literature [12,13,14]. An excellent agreement is observed over the range 10–100 of Reynolds number.

The drag coefficient is an integral quantity and its prediction does not generally imply a correct prediction of the flow field. One of the hardest tests is the prediction of pressure distribution around the sphere. The accuracy of the method is demonstrated by the pressure coefficient trend as a function of the angular coordinate, θ, shown in Fig. 4 for Re = 100. The agreement with the numerical data found in the literature [14] is excellent.

4. Conclusions

Summarizing, the ULBE method shows significant potential for the accurate calculation of flows in complex geometries. Its crucial asset is the on-line availability of the kinetic tensor, which provides two crucial advantages over hydrodynamic techniques, namely: (i) there is no need to solve the Poisson problem to obtain the fluid pressure, (ii) there is no need to take space-derivatives to compute the stress tensor.

In order to fully capitalize on the above assets, further upgrades of the time-stepping procedure are needed.

References

[1] Benzi R, Succi S, Vergassola M. The lattice Boltzmann

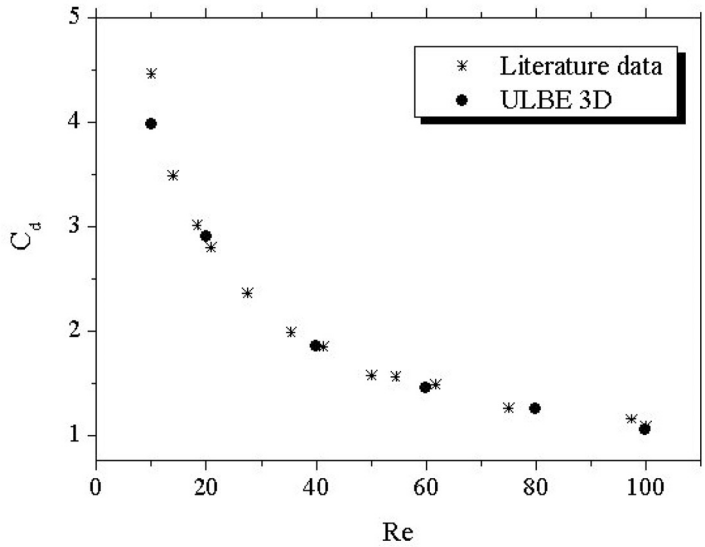

Fig. 3. Computed drag coefficient over the range 10–100 of Reynolds number and comparison with literature data [14].

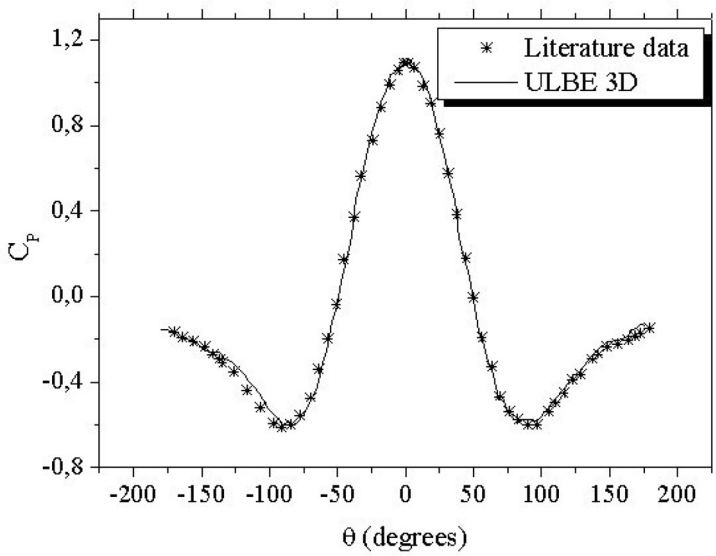

Fig. 4. Comparison between the numerically calculated pressure coefficient profile and literature data at Re = 100.

equation: theory and applications. Phys Rep 1992;222:145–197.

[2] Succi S. The Lattice Boltzmann Equation for Fluid Dynamics and Beyond. Oxford: Clarendon, 2001.

[3] Rothman DH, Zaleski S. Lattice-gas model of phase separation: interfaces, phase transitions, and multiphase flow. Rev Mod Phys 1994;66(4):1417–1479.

[4] Watanabe T, Ebihara K. Numerical simulation of coalescence and breakup of rising droplets. Comput Fluids 1994;32:823–834.

[5] Nannelli F, Succi S. The lattice Bolztmann equation on irregular lattices. J Stat Phys 2000;68:401.

[6] Filippova O, Hanel D. Grid refinement for lattice-BGK models. J Comp Phys 1998;147:219.

[7] Mei R, Shyy W. On the finite difference-based lattice Boltzmann method in curvilinear coordinates. J Comp Phys 1998;143:426.

[8] Peng G, Xi H, Duncan G, Chou SH. Lattice Boltzmann method on irregular meshes. Phys Rev E 1998;58(4):4124–4127.

[9] Ubertini S, Bella G, Succi S. Unstructured lattice

Boltzmann method: further developments. Phys Rev E 2003;68:016701.

[10] Ubertini S, Succi S, Bella G. Lattice Boltzmann schemes without coordinates. Phil Trans Royal Soc London: Math Phys Eng Sci 2004;362(1821):1763–1771.

[11] Bhatnagar P, Gross E, Krook M. A model for collision processes in gases I: small amplitude processes in charged and neutral one-component system. Phys Rev 1954;94:511.

[12] Johnson TA, Patel VC. Flow past a sphere up to a Reynolds number of 300. J Fluid Mech 1999;378:19–70.

[13] Mittal RA. Fourier-Chebyshev spectral collocation method for simulating flow past spheres and spheroids. Int J Numer Methods Fluids 1999;30:921–937.

[14] Mansoorzadeh S, Pain CC, de Oliveira CRE, Goddard AJH. Finite element simulations of incompressible flow past a heated/cooled sphere. Int J Numer Methods Fluids 1999;28:903–915.